7 **The 4.2 ka event: multi-proxy records from a closed lake in the northern**

8 **margin of the East Asian summer monsoon**

11 **Jule Xiao[1,2,3], Shengrui Zhang[1], Jiawei Fan[1], Ruilin Wen[1,2], Dayou Zhai[4], Zhiping Tian[5],**

12 **and Dabang Jiang[5]**

15 [1]CAS Key Laboratory of Cenozoic Geology and Environment, Institute of Geology and

16 Geophysics, Chinese Academy of Sciences, Beijing 100029, China

17 [2]CAS Center for Excellence in Life and Paleoenvironment, Beijing 100044, China

18 [3]College of Earth and Planetary Sciences, University of Chinese Academy of Sciences,

19 Beijing 100049, China

20 [4]School of Resources, Environment and Geosciences, Yunnan University, Kunming 650091,

21 China

22 [5]Nansen–Zhu International Research Centre, Institute of Atmospheric Physics, Chinese

23 Academy of Sciences, Beijing 100029, China

26 Correspondence: Jule Xiao (jlxiao@mail.iggcas.ac.cn)

27

28

29

30   **Abstract.** The 4.2 ka event has been widely investigated since it was suggested to be a

31   possible cause for the collapse of ancient civilizations. With the growth of proxy records for

32   decades, however, both its nature and its spatial pattern have become controversial. Here we

33   examined multi-proxy data of the grain-size distribution, ostracode assemblage, pollen

34   assemblage and the pollen-reconstructed mean annual precipitation from a sediment core at

35   Hulun Lake in northeastern Inner Mongolia spanning the period between 5000 and 3000 cal.

36   yr BP to identify the nature and the associated mechanism of the 4.2 ka event occurring in the

37   monsoonal region of eastern Asia. Higher sand fraction contents, littoral ostracodes

38   abundances and Chenopodiaceae pollen percentages together with lower mean annual

39   precipitations reveal a significant dry event at the interval of 4230–3820 cal. yr BP that could

40   be a regional manifestation of the 4.2 ka event in the northern margin of the East Asian

41   summer monsoon (EASM). We suggest that the drought would be caused by a large decline

42   in the intensity of the EASM on millennial-to-centennial scales that could be physically

43   related to persistent cooling of surface waters in the western tropical Pacific and the North

44   Atlantic. The cooling of western tropical Pacific surface waters could reduce moisture

45   productions over the source area of the EASM, while the cooling of North Atlantic surface

46   waters could suppress northward migrations of the EASM rainbelt, both leading to a

47   weakened EASM and thus decreased rainfall in the northern margin of the EASM.

48

49

50

51

52

53

54

55

56

57

58

59

1 Introduction

The 4.2 ka event has attracted worldwide interest since two articles published in the periodical Science (Weiss and Bradley, 2001; deMenocal, 2001) demonstrated that the drought that occurred 4.2 ka ago could be a possible cause for the collapse of ancient civilizations. Judging from the viewpoint of the history of paleoclimate research, however, almost no special attention had been paid to the 4.2 ka event prior to the publication of the two highlighted articles when the Holocene climatic instability had become an increasingly hot topic in the field of paleoclimatology.

In early 1990s when an oxygen isotope record for the Greenland Ice-core Project (GRIP) Summit ice core has just come out, the Holocene climate was viewed as extremely stable in contrast with large, abrupt climate changes during both the last two glaciations and the last interglacial (Dansgaard et al., 1993). In 1995, however, concentrations of sea salt and terrestrial dusts from the same ice core demonstrated that the Holocene climate of Greenland was punctuated by 4 times of millennial-scale shifts during the periods of 8800–7800, 6100–5000, 3100–2400 and 600–0 yr ago (O'Brien et al., 1995). Subsequently in 1997, an integrated Holocene climatic record of accumulation rate, δ^{18}O-based temperature, chloride and calcium concentrations, fire frequency and methane concentration for the Greenland Ice Sheet Project II (GISP2) ice core revealed a cold event that occurred between 8.4 and 8.0 ka ago, typically peaking at 8.25 cal. ka BP (Alley et al., 1997). This was first to put forward a prominent, widespread climatic event for the warm Holocene, i.e., the 8.2 ka event. In any case, however, no clear signals of the 4.2 ka event had been identified in the ice-core records from Greenland.

Encouraged by the findings of O'Brien et al. (1995), Bond et al., (1997) launched an investigation of deep-sea sediments in the North Atlantic and detected a series of abrupt shifts that punctuated the Holocene climate through studies on ice-rafted debris in the sediments. These abrupt climate events seemingly occurred at a cyclicity of 1470±500 yr during the Holocene, which did not generate any particularity for the 4.2 ka event. Taking the paleoclimatic record of Greenland ice cores together, the 4.2 ka event appears to be unexceptional for the Holocene climate in high latitudes of the Northern Hemisphere.

90   As early as in 1990s, in fact, the 4.2 ka event was first explained as a possible

91   contributor to the collapse of ancient civilization (Weiss et al., 1993). Weiss et al. (1993)

92   identified a marked increase in aridity and wind circulation occurring in northern

93   Mesopotamia at 2200 BC based on studies of archaeological sites on alluvial plains of the

94   Tigris and Euphrates Rivers, suggesting that the abrupt climatic change induced a considerable

95   degradation of land-use conditions and thus caused the collapse of the rain-fed agriculture

96   civilization of western Asia. Years later, the above-mentioned two articles (Weiss and Bradley,

97   2001; deMenocal, 2001) demonstrated that the drought that occurred 4.2 ka ago could explain

98   the societal collapse of Old World civilizations based on existing archaeological and

99   paleoclimatic data. This point of view has promoted extensive investigations into the causal

100   relationship between cultural evolution and climate change on archaeological records and also

101   drawn much attention from paleoclimatologists to researches of the 4.2 ka event. With the

102   accumulation of proxy records, however, both the nature of the 4.2 ka event (Marchant and

103   Hooghiemstra, 2004, Magny et al., 2009) and the manner of societal responses to climate

104   change (Drysdale et al., 2006; Staubwasser and Weiss, 2006) have become increasingly

105   controversial.

106   Researches on the 4.2 ka event and its impact on cultural evolution in China have been

107   motivated by Hsü's view that famines and mass migrations occurring in ancient China could

108   have resulted from regional droughts related to global cooling (Hsü, 1998). Wu and Liu (2004)

109   synthesized data from paleoclimatic records in eastern China and suggested that the climatic

110   anomaly that occurred ~4.2 ka ago produced a drought in the north and flooding in the south,

111   which was responsible for the collapse of neolithic cultures in the central plain of China

112   during the late third millennium BC. Liu and Feng (2012) recently examined the newly

113   published data of paleoclimatic and archaeological records spanning the transition from the

114   middle to late Holocene and offered a different interpretation from that of Wu and Liu (2004).

115   In brief, an abrupt climatic shift occurred in northern China at ~4 cal. ka BP; while in

116   southern China the ~4 cal. ka event had several effects. With the associated climatic drying at

117   ~4 cal. ka BP, Chinese Neolithic cultures both in the north and in the south collapsed; while

118   the Longshan Culture in the central plain thrived.

119   Here we examined the paleoclimatic data from a sediment core at Hulun Lake in

120   northeastern Inner Mongolia and focused on the research of the 4.2 ka event occurring in the

121   lake region. Hulun Lake is located in the northern margin of the East Asian summer monsoon

122   that represents a climatically sensitive zone. The multi-proxy paleoclimatic records from the

123   lake would provide new insights into the 4.2 ka event. This study is aimed to identify the

124   nature and the associated mechanism of the 4.2 ka event occurring in the monsoonal region of

125   eastern Asia.

126

127   **2 Study site**

128

129   Hulun Lake (48°30.667' to 49°20.667'N, 117°0.167' to 117°41.667'E), the fifth largest

130   lake in China, is situated about 30 km south of Manchuria, Inner Mongolia, China (Fig. 1). It

131   lies in an inland graben basin that was formed in the late Pliocene (Xu et al., 1989). It has an

132   area of 2339 km^2 and a maximum water depth of 8 m when the lake level attains to the

133   highest status at an elevation of 545.3 m a.s.l. (measurements in August 1964; Xu et al., 1989).

134   Today, the lake is closed and the maximum water depth is 5 m (Fig. 1). Low mountains and

135   hills of Mesozoic volcanic rocks border the lake on the northwest and form a fault-scarp

136   shoreline. Broad lacustrine and alluvial plains extend from the southern and eastern shores of

137   the lake with scattered aeolian dunes. The lake has a catchment of 37,214 km^2 within the

138   borders of China. Two rivers, the Herlun from the southwest and the Urshen Rivers from the

139   southeast, supply water for the lake (Fig. 1). The Dalanolom River, an intermittent river to the

140   northeast of the lake, drains the lake when the elevation of the lake level exceeds 543.4 m a.s.l.

141   and enters the lake when the lake level is lower and the discharge of the Hailar River is larger

142   as well (Xu et al., 1989) (Fig. 1).

143   Hulun Lake is located in a semi-arid area of the middle temperate zone (Fig. 1). The

144   climate of the lake's region is influenced by the East Asian monsoon and the Westerlies

145   (Chinese Academy of Sciences, 1984; Zhang and Lin, 1985). During summer, warm, moist

146   southerly air-masses interact with cold air from the northwest and produce most of the annual

147   precipitation. During winter, cold, dry northwesterly airflows prevail and generate strong

148   winds and cold weathers. In the lake region, mean annual temperature is 0.3℃ with a July

149   average of 20.3℃ and a January average of –21.2℃. Annual precipitation is 247 to 319 mm,

150   and over 80% of the annual precipitation falls in June–September. Annual evaporation

151   reaches 1400 to 1900 mm, which is ~6 times the annual precipitation. The lake is covered

152   with ~1 m of ice from November to April.

153   The ostracodes living in the lake today include *Limnocythere inopinata* (Baird),

154   *Candoniella suzini* Schneider, *Pseudocandona albicans* (Brady), *Pseudocandona compressa*

155   (Koch), *Cyclocypris serena* (Koch), *Ilyocypris gibba* (Ramdohr) and *Ilyocypris salebrosa*

156   Stepanaiths (Xu et al., 1989; Wang and Ji, 1995). *Limnocythere inopinata* is the dominant

157   species. Aquatic plants are scarce in the lake and confined to the areas of the river mouth and

158   parts of the nearshore zone.

159   The modern natural vegetation of the lake basin belongs to the middle temperate steppe

160   (Compilatory Commission of Vegetation of China, 1980; Xu et al., 1989). The vegetation

161   cover ranges from relatively moist forb-grass meadow-steppe in the piedmont belt to

162   moderately dry grass steppe on the alluvial plain and dry bunchgrass–undershrub *Artemisia*

163   steppe on the lacustrine plain. Halophilic Chenopodiaceae plants are distributed in the

164   lowlands. The forests are developed on the west slopes of the Great Hinggan Range, where

165   the Urshen and Hailar River rise, accompanied by scrubs and herbs under the trees. Larch

166   forests cover the southern part of the Hentiy Mountains where the Herlun River rises. Patches

167   of pine forests and birch shrubberies occur in the alpine belt.

168

169   **3 Material and methods**

170

171   3.1 Lithology and chronology of the HL06 core

172

173   Drilling was conducted at a water depth of 5 m in the central part of Hulun Lake in

174   January 2006 when the lake was frozen (Fig. 1), using a TOHO drilling system. A sediment

175   core was extracted to a depth beneath the lake floor of 1.7 m and is designated HL06

176   (49°07.615' N, 117°30.356' E; Fig. 1). The core section was split, photographed and described

177   on site and then cut into 1-cm segments, resulting in 170 samples for laboratory analyses.

178   The sediments of the HL06 core can be divided into three parts: 1) upper blackish-grey

179   oozy mud at depths of 0–35 cm, 2) middle dark grey to blackish-grey, massive sandy mud

180   with scattered fragments of ostracodes and mollusk shells at depths of 35–100 cm, and 3)

181   lower greenish-grey homogeneous mud at depths of 100–170 cm (Xiao et al., 2009).

182   Thirteen bulk samples were collected from organic-rich horizons of the HL06 core and

183   dated with an Accelerator Mass Spectrometry (AMS) system (Compact-AMS, NEC

184   Pelletron) at Paleo Labo Co., Ltd. in Japan. As shown in Xiao et al. (2009), the uppermost 0–1

185   cm of the core sediments yields a ^{14}C age of 685±21 yr that was considered to result from

186   carbon reservoir effects on radiocarbon dating of the bulk organic matter of Hulun Lake

187   sediments. To produce an age–depth model for the HL06 core, the carbon reservoir age of

188   685±21 yr was first subtracted from all the original ^{14}C ages, and then calibrations are

189   performed on the carbon reservoir-free ^{14}C ages. The conventional ages were converted to

190   calibrated ages using the OxCal3.1 radiocarbon age calibration program (Bronk Ramsey,

191   2001) with the IntCal04 calibration data (Reimer et al., 2004). The age–depth model indicates

192   that the HL06 core covers the last ~11,000 yr (Xiao et al., 2009).

193

194   3.2 Proxy analyses of the HL06 core

195

196   The HL06 core has been analysed at 1-cm interval for multiple proxies including

197   grain-size distribution (Xiao et al., 2009), ostracode assemblage (Zhai et al., 2011), and pollen

198   assemblage (Wen et al., 2010a) in order to investigate the Holocene history of changes in the

199   hydrology of Hulun Lake and in vegetation and climate of the lake region. Grain-size

200   distribution was determined with a Malvern Mastersizer 2000 laser grain-size analyzer (Xiao

201   et al., 2009). Each sample of sediment was pretreated with hydrogen peroxide to remove

202   organic matter and then with boiled hydrochloric acid to remove carbonates. The sample

203   residue was dispersed with sodium metaphosphate on an ultrasonic vibrator before grain-size

204   analysis.

205   For the ostracode assemblage analysis, each sample of ~300 mg of air-dried sediment

206   was pretreated with hydrogen peroxide–sodium carbonate solution (pH 9–10) to disaggregate

207   the sediment (Zhai et al., 2011). Fossil ostracode valves were extracted by sieving in water

208   through a 250-mesh sieve (63-μm pore size). Ostracode was identified and counted from the

209   sieve residue spread onto a glass plate with an Olympus stereomicroscope at 40×

210   magnifications following the taxonomy of Meisch (2000) and Hou et al. (2002). Most

211   samples yielded 300 to 4000 ostracode valves.

212   For the pollen assemblage analysis, each sample of ~1 g of air-dried sediment was

213   pretreated with hydrochloric acid to remove carbonates and with sodium hydroxide to remove

214   organic matter; the residue was then kept in hydrofluoric acid to remove silicates (Wen et al.,

215   2010a). Fossil pollen grains were extracted by wet sieving of the resulting residue through a

216   sieve diameter of 10 μm with an ultrasonic cleaner. Pollen was identified and counted with an

217   Olympus light microscope at 400× magnifications. More than 600 pollen grains were counted

218   for each sample. The percentages of tree and herb pollen taxa were based on the sum of the

219   total terrestrial pollen in a sample, and those of each taxon of both aquatic pollen and fern

220   spores based on the sum of the terrestrial pollen plus the aquatic pollen or fern spores of the

221   taxon in a sample.

222   In addition, the history of changes in precipitation in the Hulun Lake region during the

223   Holocene was quantitatively reconstructed (Wen et al., 2010b) based on the pollen profile of

224   the HL06 core (Wen et al., 2010a), using a pollen–climate transfer function for temperate

225   eastern Asia (Wen et al., 2013).

226

227   3.3 Proxy data from the HL06 core used for the present study

228

229   The segment of the HL06 core spanning the period between 5000 and 3000 cal. yr BP is

230   used for the present study to focus on the research of the 4.2 ka event occurring in the Hulun

231   Lake region. Fig. 2 shows the lithology and ages of the core segment between 105 and 55 cm

232   at depth, which covers the segment between dated horizons of a calibrated age older than

233   5000 cal. yr BP and of a calibrated age younger than 3000 cal. yr BP. Ages of sampled

234   horizons of the core segment spanning the period of 5000–3000 cal. yr BP were derived by

235   linear interpolation between radiocarbon-dated horizons using the mean values of 2σ   ranges

236   of calibrated ages.

237   Data of grain-size distribution (Xiao et al., 2009), ostracode assemblage (Zhai et al.,

238   2011), pollen assemblage (Wen et al., 2010a), and mean annual precipitation (Wen et al.,

239   2010b) from the HL06 core for the period of 5000–3000 cal. yr BP were re-examined in the

240   present study in order to explore the detailed process of climate changes on

241   millennial-to-centennial scales in the Hulun Lake region around 4.2 cal. ka BP.

242

243   **4 Results**

244

245   The sediments of the core segment spanning the period of 5000–3000 cal. yr BP consist

246   of dark grey to blackish-grey, massive sandy mud in which the scattered fragments of

247   ostracode and mollusk shells can be seen (Fig. 2). Five radiocarbon dates provide age controls

248   for the core segment spanning the period of 5000–3000 cal. yr BP (corresponding to the core

249   depths of 97–68 cm) (Fig. 2; Table 1). Data of sand fraction content, littoral ostracodes

250   abundance, Chenopodiaceae pollen percentage, and mean annual precipitation from the core

251   segment spanning the period of 5000–3000 cal. yr BP were plotted against age in Figure 3.

252

253   4.1 Sand fraction content

254

255   The content of the sand fraction in the core sediments has an average of 7.5% for the

256   period of 5000–3000 cal. yr BP (Fig. 3). At the interval of 4560–3820 cal. yr BP (core depth:

257   92.0–82.5 cm), the sand fraction content shows higher-than-average values with a maximum

258   of 21.1% and an average of 15.0% (Fig. 3).

259

260   4.2 Littoral ostracodes abundance

261

262   The abundance of the littoral ostracodes including *Pseudocandona albicans*,

263   *Pseudocandona* sp., *Candoniella subellipsoida*, and *Cypridopsis* sp. from the core sediments

264   has an average of 22 valves g^{-1} for the period of 5000–3000 cal. yr BP (Fig. 3). At the interval

265   of 4380–3380 cal. yr BP (core depth: 90.0–75.5 cm), the littoral ostracodes abundance shows

266   higher-than-average values with a maximum of 70 valves g^{-1} and an average of 40 valves g^{-1}

267   (Fig. 3).

268

269   4.3 Chenopodiaceae pollen percentage

270

271   The percentage of Chenopodiaceae pollen from the core sediments has an average of

272   42.9% for the period of 5000–3000 cal. yr BP (Fig. 3). At the interval of 4610–3460 cal. yr

273   BP (core depth: 92.5–77.0 cm), the Chenopodiaceae pollen percentage shows

274   higher-than-average values with a maximum of 60.2% and an average of 51.3% (Fig. 3).

275

276   4.4 Mean annual precipitation

277

278   The mean annual precipitation in the lake region reconstructed on the pollen profile of

279   the sediment core has an average of 297.3 mm for the period of 5000–3000 cal. yr BP (Fig. 3).

280   At the interval of 4580–3580 cal. yr BP (core depth: 92.0–79.5 cm), the mean annual

281   precipitation shows lower-than-average values with a minimum of 264.0 mm and an average

282   of 278.2 mm (Fig. 3).

283

284   **5 Discussion**

285

286   5.1 Climatic implication of proxy data from the HL06 core

287

288   Grain-size distributions of the core sediments show that the clay, silt and sand fractions

289   average 35.8%, 60.6% and 3.6% of the clastic materials during the Holocene, respectively

290   (Xiao et al., 2009). Sand grains from the nearshore zone of Hulun Lake could be transported

291   to and deposited in the central part of the lake when the lake assumed low stands. Therefore

292   increases in the relative percentage of the sand fraction in the core sediments were interpreted

293   to indicate drops in the water level of Hulun Lake (Xiao et al., 2009). We thus infer that

294   higher values of the sand fraction content at the interval of 4560–3820 cal. yr BP imply

295   relatively lower lake levels at that time (Fig. 3).

296   Ostracode assemblages of the core sediments suggest that fourteen species of ostracodes

297   belonging to nine genera occur in Hulun Lake during the Holocene and *Limnocythere*

298   *inopinata* is the dominant species (Zhai et al., 2011). *Pseudocandona albicans*,

299   *Pseudocandona* sp., *Candoniella subellipsoida*, and *Cypridopsis* sp. from the core sediments

300   were interpreted as littoral ostracode taxa because these ostracodes usually live in small water

301   bodies and shallow waters and have a wide tolerance to water temperature or salinity (Zhai et

302   al., 2011). We thus infer that higher values of the littoral ostracodes abundance at the interval

303   of 4380–3380 cal. yr BP imply relatively lower lake levels at that time (Fig. 3).

304   Pollen assemblages of the core sediments suggest that dry grass steppe dominated by

305   *Artemisia* and Chenopodiaceae plants were developed in the Hulun Lake basin during most of

306   the Holocene (Wen et al., 2010a). In the modern steppe of northern China, Chenopodiaceae

307   predominates over *Artemisia* in the desert steppe as compared with in the typical steppe.

308   Therefore increases in the relative percentage of Chenopodiaceae pollen in the core sediments

309   were interpreted to indicate decreases in the effective moisture in the lake basin (Wen et al.,

310   2010a). We thus infer that higher values of the Chenopodiaceae pollen percentage at the

311   interval of 4610–3460 cal. yr BP imply relatively lower effective moistures in the lake basin

312   at that time (Fig. 3).

313   The pollen-reconstructed mean annual precipitation yields a value of around 285 mm in

314   the Hulun Lake region for the last decades (Wen et al., 2010b). This value of the mean annual

315   precipitation falls within the range of observed data of the annual precipitation (247–319 mm),

316   demonstrating the validity of the pollen–climate transfer function in quantitatively

317   reconstructing the regional precipitation. Therefore lower values of the mean annual

318   precipitation at the interval of 4580–3580 cal. yr BP denote relatively drier conditions in the

319   lake basin at that time (Fig. 3).

320

321   5.2 The nature and timing of the 4.2 ka event in the Hulun Lake region

322

323   As remarked above, the sand fraction content and the littoral ostracodes abundance of

324   the lake sediments can be used as indicators of changes in the lake level that is closely related

325   to changes in the water balance (precipitation plus runoff minus evaporation) of the lake; while

326   the Chenopodiaceae pollen percentage can be used as a direct indicator of changes in the

327   effective moisture in the lake basin. The mean annual precipitation can directly indicate

328   changes in the amount of precipitation in the lake basin. During the period of 5000–3000 cal.

329   yr BP, data of the sand fraction content, littoral ostracodes abundance, Chenopodiaceae pollen

330   percentage, and the mean annual precipitation can be well correlated with each other,

331   although the intervals of a relatively drier climate in the lake basin registered by different

332   proxies differ slightly in the time of start and end (Fig. 3).

333   In order to detect the pattern of temporal changes in the regional dry–wet condition

334   during the period of 5000–3000 cal. yr BP, principle component analysis (PCA) was

335   performed to analyze the time series of data of the sand fraction content, littoral ostracodes

336   abundance, Chenopodiaceae pollen percentage, and the mean annual precipitation. All the raw

337   data of the 4 proxies were standardized, and then PCA was conducted on the standardized

338   data with the proxies as variables. F1, F2 and the first three factors of PCA capture 74.5%,

339   15.4% and 97.9% of the total variance within the data set, respectively. As shown in Figure 3,

340   PCA F1 with an average of 0 for the period of 5000–3000 cal. yr BP displays

341   higher-than-average values at the interval of 4540–3480 cal. yr BP (core depth: 92.0–77.5 cm)

342   with a maximum of 1.71 and an average of 0.88.

343   PCA F1 reflects the common characteristics of the aforementioned four proxies for the

344   relatively drier climate in the lake region at the interval of 4540–3480 cal. yr BP.

345   Discrepancies in both the timing of the relatively drier interval from each proxy and the detail

346   of different proxies on centennial to multi-decadal scales within the interval can be explained

347   by differences in the response of different proxies to changes in the regional precipitation and

348   the lake's hydrology. We thus suggest that the climatic drying occurring in the Hulun Lake

349   basin could be the regional manifestation of the 4.2 ka event.

350   In order to delimitate a dry event from the relatively drier climate at the interval of

351   4540–3480 cal. yr BP reflected by PCA F1, we define a central interval at which PCA F1

352   displays values that are larger than its average for the interval of 4540–3480 cal. yr BP (0.88).

353   This central interval started at 4230 cal. yr BP and ended at 3820 cal. yr BP with duration of

354   410 yr, which exactly delineates a peak interval for each of the four proxies (Fig. 3). We thus

355   suggest that the dry event corresponding to the 4.2 ka event occurred in the Hulun Lake

356   region at 4230–3820 cal. yr BP and lasted for 410 yr.

357

358   5.3 Possible cause of the 4.2 ka event in the Hulun Lake region

359

360   Hulun Lake is situated in the northern marginal zone of the East Asian summer

361   monsoon (EASM) (Fig. 1). Modern observations indicate that precipitation in the Hulun Lake

362   region reaches its peak value in July and ~70% of the annual precipitation falls in late June

363   through early August (Xu et al., 1989). Changes in the precipitation of the lake region in the

364   summer half-year totally follow the northward migrations of the EASM rainbelt (Fig. 4),

365   indicating that increases in the precipitation of the lake region would be closely related to

366   increases in the strength of the EASM. These data suggest that the dry event that occurred in

367   the Hulun Lake region at 4230–3820 cal. yr BP implies a large decline of the EASM.

368   The northward migrations of the EASM rainbelt in rainy seasons of East Asia are

369   characterized by two discontinuous jumps (i.e., jumping first to the Yangtse River–Huaihe

370   River basin, southwestern Japan and southern Korea in late June and then to northern China,

371   northeastern China and northern Korea in middle July after landing in southern China in late

372   May) (Fig. 4), which are influenced not only by the ocean–atmosphere interactions in the

373   tropical Pacific because the moisture/rainfall brought by the EASM onto the land derives

374   from the western tropical Pacific but also by the pattern of atmospheric circulation over

375   Northern Hemisphere high latitudes because the EASM frontal rainfall results from the

376   interaction between the warm-moist, southerly air-masses and the cold-dry, northwesterly

377   airflows (Chinese Academy of Sciences, 1984; Zhang and Lin, 1985). In Figure 5, therefore,

378   dry–wet oscillations in the Hulun Lake region reflected by PCA F1 for the period of 5000–

379   3000 cal. yr BP are compared with the sea-surface-temperature (SST) record from the western

380   tropical Pacific (Stott et al., 2004) and the hematite-stained-grains (HSG) record from the

381   North Atlantic (Bond et al., 2001).

382   As shown in Fig. 5, the large decline of the EASM occurring at 4230–3820 cal. yr BP

383   coincides, within age uncertainties, with decreases in the SST of the western tropical Pacific

384   (Stott et al., 2004) and with increases in the HSG concentration in the North Atlantic

385 sediments (Bond et al., 2001). This coincidence implies a physical link between the EASM

386 decline on millennial-to-centennial scales and the persistent cooling of surface waters of the

387 western tropical Pacific as well as the North Atlantic. In brief, continual decreases in sea

388 surface temperature of the western tropical Pacific presumably caused by more intense, more

389 frequent El Niño (Moy et al., 2002) could reduce the formation of water vapor over the source

390 area of the EASM, thereby decreasing the moisture available for transport via the EASM

391 circulation from the western tropical Pacific onto the Asian inland and leading to a weakened

392 EASM. While decreases in sea surface temperature of the North Atlantic could suppress the

393 northward migration of the EASM front, thereby hampering the northward jumps of the

394 EASM rainbelt and resulting in weakened rainfall in the northern marginal zone of the

395 EASM.

396

397 **6. Conclusions**

398

399 Multiple proxies of a sediment core at Hulun Lake in northeastern Inner Mongolia

400 reveal a prominent dry event occurring at the interval of 4230–3820 cal. yr BP that could be

401 the regional manifestation of the 4.2 ka event in the northern marginal zone of the EASM. The

402 drought would have resulted from a large decline of the EASM that could be physically linked

403 with the persistent cooling of surface waters of the western tropical Pacific and the North

404 Atlantic on millennial-to-centennial scales.

405 Although more and more proxy data have been obtained, an integrated view of the 4.2

406 ka event is still far beyond reach. Future studies should be focused on the investigation of

407 high-quality, high-resolution proxy records from more, climatically sensitive and

408 geographically representative regions in order to explore the spatiotemporal pattern of the 4.2

409 ka event and the associated dynamic mechanism.

410

411 **Acknowledgments**

412

413   This study was financially supported by the National Key R&D Program of China

414   (Grant 2017YFA0603400) and the National Natural Science Foundation of China (Grant

415   41130101).

416

417

418

419   **References**

420

421   Alley, R. B., Mayewski, P. A., Sowers, T., Stuiver, M., Taylor, K. C., and Clark, P. U.:

422   Holocene climatic instability: A prominent, widespread event 8200 yr ago, Geology, 25,

423   483–486, 1997.

424   Bond, G., Showers, W., Cheseby, M., Lotti, R., Almasi, P., deMenocal, P., Priore, P., Cullen,

425   H., Hajdas, I., and Bonani, G.: A pervasive millennial-scale cycle in North Atlantic

426   Holocene and glacial climates, Science 278, 1257–1266, 1997.

427   Bond, G., Kromer, B., Beer, J., Muscheler, R., Evans, M. N., Showers, W., Hoffmann, S.,

428   Lotti-Bond, R., Hajdas, I., and Bonani, G.: Persistent solar influence on North Atlantic

429   climate during the Holocene, Science, 294, 2130–2136, 2001.

430   Bronk Ramsey, C.: Development of the radiocarbon calibration program, Radiocarbon, 43,

431   355–63, 2001.

432   Chinese Academy of Sciences (Compilatory Commission of Physical Geography of China):

433   Physical Geography of China: Climate. Science Press, Beijing, pp. 1–30, 1984 (in

434   Chinese).

435   Compilatory Commission of Vegetation of China: Vegetation of China, Science Press,

436   Beijing, pp. 932–955, 1980 (in Chinese).

437   Dansgaard, W., Johnsen, S. J., Clausen, H. B., Dahl-Jensen, D., Gundestrup, N. S., Hammer,

438   C. U., Hvidberg, C. S., Steffensen, J. P., Sveinbjörnsdottir, A. E., Jouzel, J., and Bond,

439   G.: Evidence for general instability of past climate from a 250-kyr ice-core record,

440   Nature, 364, 218–220, 1993.

441   deMenocal, P. B.: Cultural responses to climate change during the late Holocene, Science,

442   292, 667–673, 2001.

443   Drysdale, R., Zanchetta, G., Hellstrom, J., Maas, R., Fallick, A., Pickett, M., Cartwright, I.,
444   and Piccini, L.: Late Holocene drought responsible for the collapse of Old World
445   civilizations is recorded in an Italian cave flowstone, Geology, 34, 101–104, 2006.

446   Hou, Y. T., Gou, Y. X., and Chen, D. Q.: Fossil Ostracoda of China (Vol. 1), Science Press,
447   Beijing, 1090 pp., 2002 (in Chinese).

448   Hsü, K. J.: Sun, climate, hunger, and mass migration, Science in China (Series D), 41, 449–
449   472, 1998.

450   Liu, F. G. and Feng, Z. D.: A dramatic climatic transition at ~4000 cal. yr BP and its cultural
451   responses in Chinese cultural domains, Holocene, 22, 1181–1197, 2012.

452   Magny, M., Vannière, B., Zanchetta, G., Fouache, E., Touchais, G., Petrika, L., Coussot, C.,
453   Walter-Simonnet, A. V., and Arnaud, F.: Possible complexity of the climatic event
454   around 4300–3800 cal. BP in the central and western Mediterranean, Holocene, 19,
455   823–833, 2009.

456   Marchant, R. and Hooghiemstra, H.: Rapid environmental change in African and South
457   American tropics around 4000 years before present: a review, Earth-Sci. Rev., 66, 217–
458   260, 2004.

459   Meisch, C.: Freshwater Ostracoda of Western and Central Europe, Spektrum, Heidelberg, 522
460   pp., 2000.

461   Moy, C. M., Seltzer, G. O., Rodbell, D. T., and Anderson, D. M.: Variability of El
462   Niño/Southern Oscillation activity at millennial timescales during the Holocene epoch,
463   Nature, 420, 162–165, 2002.

464   O'Brien, S. R., Mayewski, P. A., Meeker, L. D., Meese, D. A., Twickler, M. S., and Whitlow,
465   S. I.: Complexity of Holocene climate as reconstructed from a Greenland ice core,
466   Science, 270, 1962–1964, 1995.

467   Reimer, P. J., Baillie, M. G. L., Bard, E., Bayliss, A., Beck, J. W., Bertrand, C. J. H., Blackwell,
468   P. G., Buck, C. E., Burr, G. S., Cutler, K. B., Damon, P. E., Edwards, R. L., Fairbanks, R.
469   G., Friedrich, M., Guilderson, T. P., Hogg, A. G., Hughen, K. A., Kromer, B., McCormac,
470   G., Manning, S., Bronk Ramsey, C., Reimer, R. W., Remmele, S., Southon, J. R., Stuiver,
471   M., Talamo, S., Taylor, F. W., van der Plicht, J., and Weyhenmeyer, C. E.: Intcal04
472   terrestrial radiocarbon age calibration, 0–26 cal kyr BP, Radiocarbon, 46, 1029–58, 2004.

473   Staubwasser, M. and Weiss, H.: Holocene climate and cultural evolution in late prehistoric–

474   early historic West Asia, Quaternary Res., 66, 372–387, 2006.

475   Stott, L., Cannariato, K., Thunell, R., Haug, G. H., Koutavas, A., and Lund, S.: Decline of

476   surface temperature and salinity in the western tropical Pacific Ocean in the Holocene

477   epoch, Nature, 431, 56–59, 2004.

478   Wang, S. M. and Ji, L.: Paleolimnology of Hulun Lake, University of Science and

479   Technology of China Press, Hefei, 125 pp., 1995 (in Chinese).

480   Weiss, H., Courty, M. A., Wetterstrom, W., Guichard, F., Senior, L., Meadow, R., and

481   Curnow, A.: The genesis and collapse of third millennium north Mesopotamian

482   civilization, Science, 261, 995–1004, 1993.

483   Weiss, H. and Bradley, R. S.: What drives societal collapse? Science, 291, 609–610, 2001.

484   Wen, R. L., Xiao, J. L., Chang, Z. G., Zhai, D. Y., Xu, Q. H., Li, Y. C., Itoh, S., and Lomtatidze,

485   Z.: Holocene climate changes in the mid-high latitude monsoon margin reflected by the

486   pollen record from Hulun Lake, northeastern Inner Mongolia, Quaternary Res., 73, 293–

487   303, 2010a.

488   Wen, R. L., Xiao, J. L., Chang, Z. G., Zhai, D. Y., Xu, Q. H., Li, Y. C., and Itoh, S.: Holocene

489   precipitation and temperature variations in the East Asian monsoonal margin from

490   pollen data from Hulun Lake in northeastern Inner Mongolia, China, Boreas, 39, 262–

491   272, 2010b.

492   Wen, R. L., Xiao, J. L., Ma, Y. Z., Feng, Z. D., Li, Y. C., and Xu, Q. H.: Pollen–climate

493   transfer functions intended for temperate eastern Asia, Quaternary Int., 311, 3–11, 2013.

494   Wu, W. X. and Liu T. S.: Possible role of the "Holocene Event 3" on the collapse of Neolithic

495   Cultures around the Central Plain of China, Quaternary Int., 117, 153–166, 2004.

496   Xiao, J. L., Chang, Z. G., Wen, R. L., Zhai, D. Y., Itoh, S., and Lomtatidze, Z.: Holocene weak

497   monsoon intervals indicated by low lake levels at Hulun Lake in the monsoonal margin

498   region of northeastern Inner Mongolia, China, Holocene, 19, 899–908, 2009.

499   Xu, Z. J., Jiang, F. Y., Zhao, H. W., Zhang, Z. B., and Sun, L.: Annals of Hulun Lake, Jilin

500   Literature and History Publishing House, Changchun, 691 pp., 1989 (in Chinese).

501   Zhai, D. Y., Xiao, J. L., Zhou, L., Wen, R. L., Chang, Z. G., Wang, X., Jin, X. D., Pang, Q. Q.,

502   and Itoh, S.: Holocene East Asian monsoon variation inferred from species assemblage

503   and shell chemistry of the ostracodes from Hulun Lake, Inner Mongolia, Quaternary

504   Res., 75, 512–522, 2011.

505 Zhang, J. C. and Lin, Z. G.: Climate of China, Shanghai Scientific and Technical Publishers,

506   Shanghai, 603 pp., 1985 (in Chinese).

507

508

509

510 **Figure captions**

511

512 **Figure 1.** Map of Hulun Lake (from http://www.maps.google.com) showing the location of

513 the HL06 core. The bathymetric survey of the lake was conducted in July 2005 with a FE-606

514 Furuno Echo Sounder (contours in meters). The inset gives a sketch map of China showing

515 the current northern limit of the East Asian summer monsoon (dashed line) defined as the

516 400-mm isohyet of mean annual precipitation (Chinese Academy of Sciences, 1984; Zhang

517 and Lin, 1985) and the location of Hulun Lake (solid circle). EASM shown in the inset

518 indicates the East Asian summer monsoon.

519

520 **Figure 2.** Lithological log and age–depth model of the segment of the HL06 core between

521 105 and 55 cm at core depth (covering the period between 5000 and 3000 cal. yr BP). Solid

522 circles represent the mean values of 2σ ranges of calibrated ages of carbon reservoir-corrected

523 radiocarbon dates. The carbon reservoir correction factor is 685±21 yr, ^{14}C age of the

524 uppermost 1 cm of the core sediments. Modified after Xiao et al. (2009).

525

526 **Figure 3.** Time series of sand fraction (%) (Xiao et al., 2009), littoral ostracodes valve (valves

527 g^{-1}) (Zhai et al., 2011), Chenopodiaceae pollen (%) (Wen et al., 2010a), and mean annual

528 precipitation (mm) (Wen et al., 2010b) from the HL06 core spanning the period between 5000

529 and 3000 cal. yr BP as well as the PCA F1 obtained from the aforementioned four proxies.

530 The chronology was derived from the carbon reservoir-corrected age–depth model; ages of

531 sampled horizons were determined by linear interpolation between radiocarbon-dated

532 horizons using the mean values of 2σ ranges of calibrated ages (Xiao et al., 2009). Vertical

533   dashed lines show the averages of each proxy data as well as the average of PCA F1 values

534   during the period between 5000 and 3000 cal. yr BP. Light grey bars mark the intervals at

535   which the proxy or PCA F1 has higher-than-average (lower-than-average for mean annual

536   precipitation) values. The dark grey bar superimposed on light grey bars represents the

537   interval at which PCA F1 values are higher than the average of the higher-than-average values

538   for 5000–3000 cal. yr BP.

539

540   **Figure 4.** A sketch map of eastern China, Korea and western Japan showing precipitation

541   rates of the current East Asian summer monsoon. Data are averaged by observations of the

542   years 1979–2007 and expressed in mm d^{-1} at a grid resolution of 0.25° × 0.25°. (a) On the 4th,

543   5th and 6th pentads of July and 1st pentad of August. (b) On the 5th and 6th pentads of June

544   and the 1st and 2nd pentads of July. (c) On the 5th and 6th pentads of May and the 1st and

545   2nd pentads of June.

546

547   **Figure 5.** Correlation of dry–wet oscillation in the Hulun Lake region denoted by PCA F1

548   factor from the four proxies of the HL06 core with sea-surface temperature (SST, °C)

549   reconstructed on the Mg/Ca ratio of *Globigerinoides rubber* from MD98-2176 core in the

550   western tropical Pacific (Stott et al., 2004) and hematite-stained grain concentration (HSG, %)

551   in VM29-191 core from the North Atlantic (Bond et al., 2001). The shaded bar marks an

552   interval of dry event occurring in the Hulun Lake region at 4230–3820 cal. yr BP.

553

554   **Table 1.** AMS radiocarbon dates of samples from the segment of the HL06 core between 105

555   and 55 cm at core depth (covering the period between 5000 and 3000 cal. yr BP). The

556   radiocarbon date of the uppermost 1 cm of the core sediments used for carbon reservoir

557   correction is shown. Modified after Xiao et al. (2009).

Figure 1
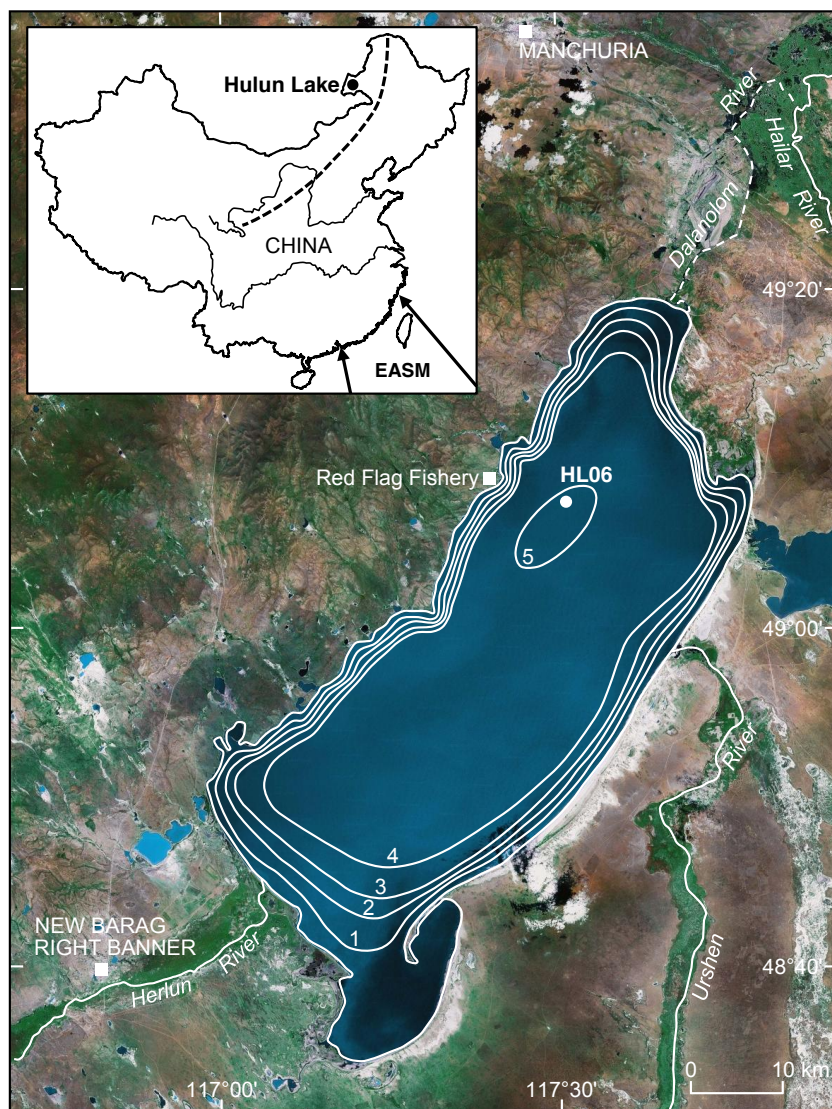
Figure 2
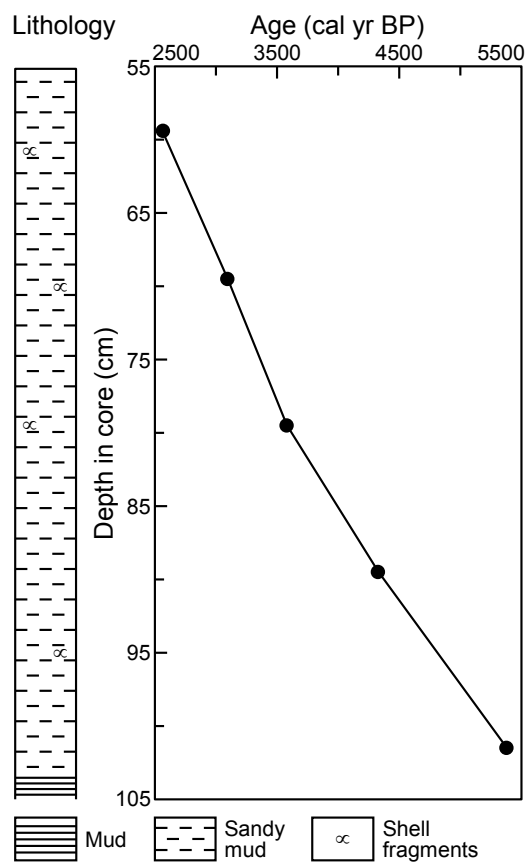
Figure 3
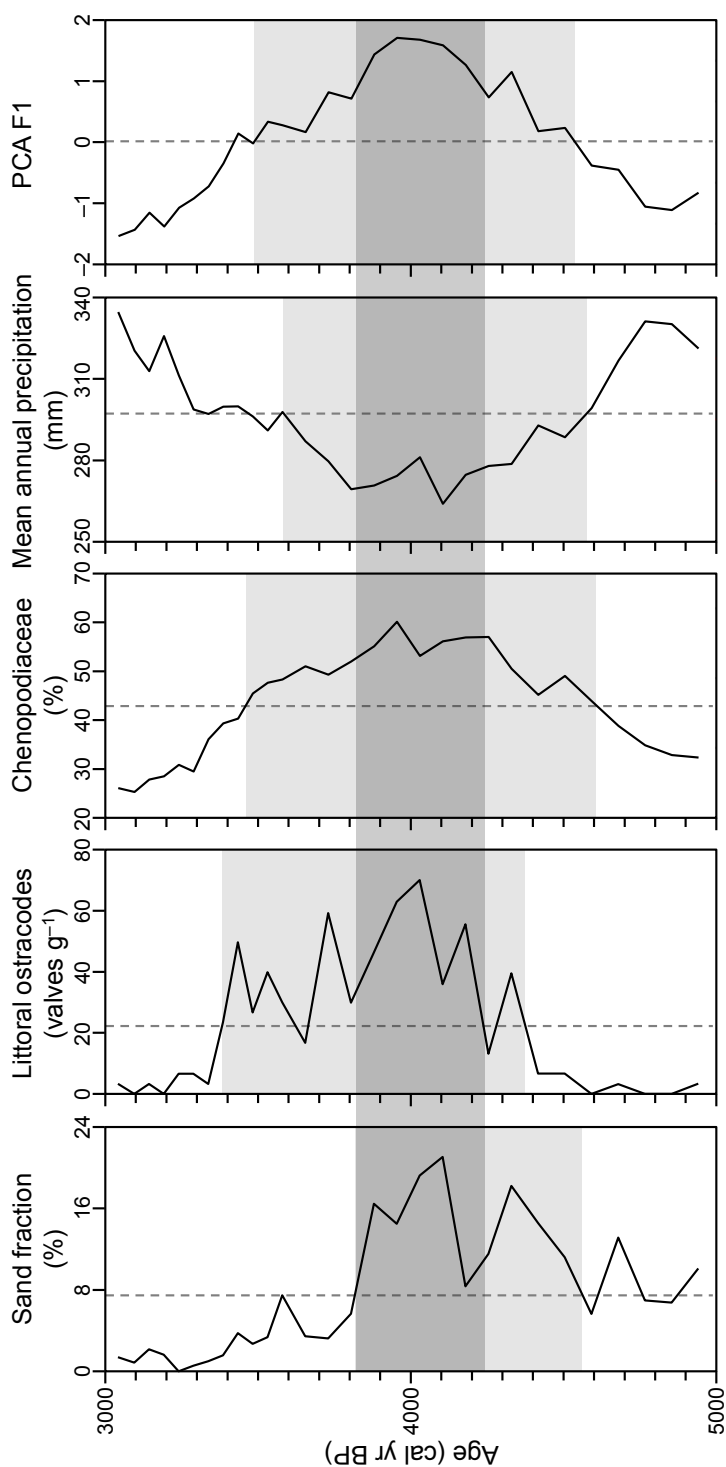
Figure 4
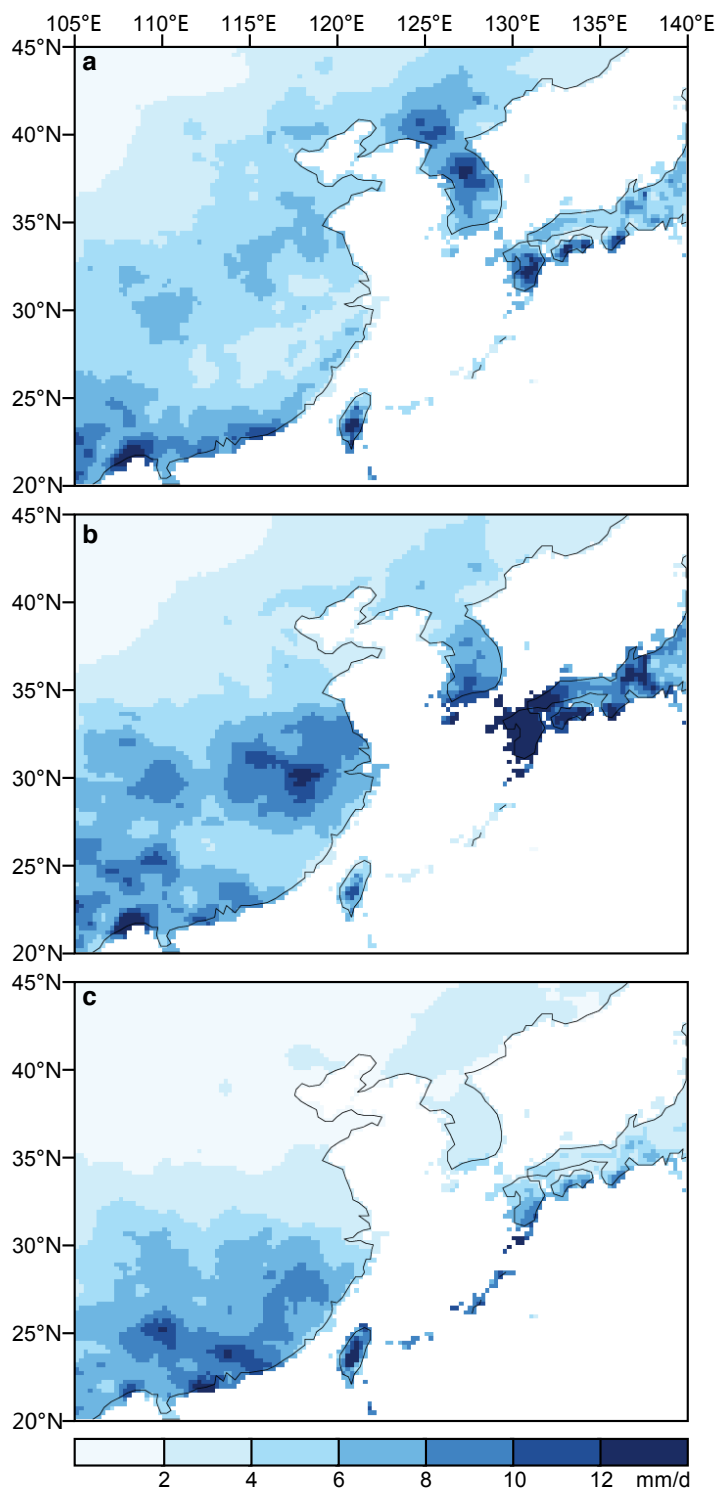
Figure 5
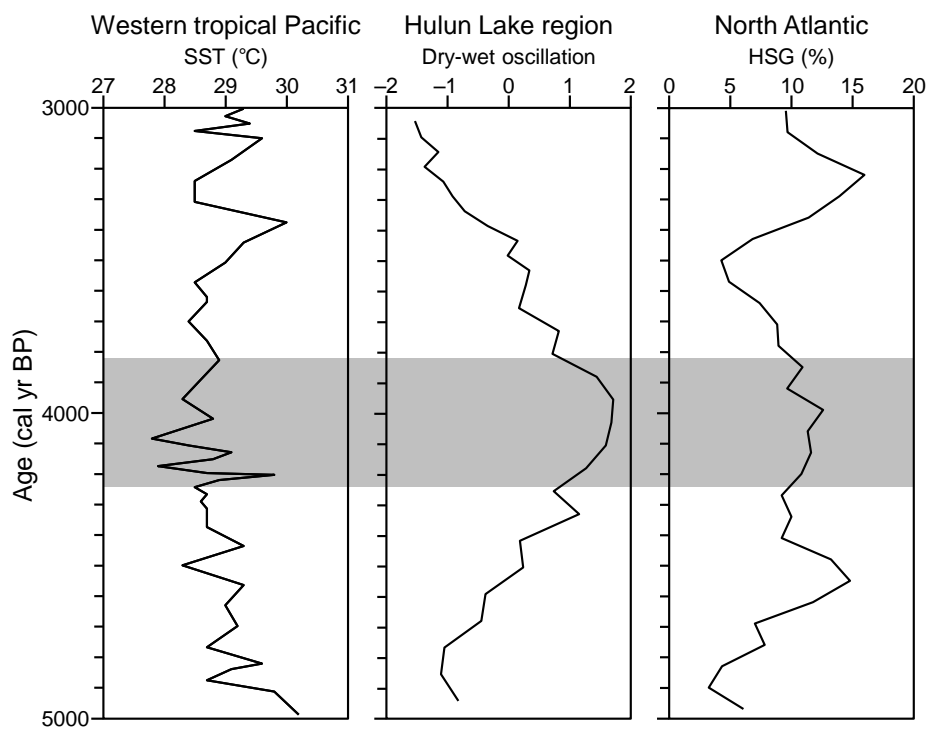
Table 1

Laboratory number[a]	Depth interval (cm)	Dating material	$\delta^{13}C$ (‰)	AMS ^{14}C age (^{14}C yr BP)	Corrected ^{14}C age[b] (^{14}C yr BP)	Calibrated ^{14}C age (2σ) (cal yr BP)
PLD-7489	0–1	Organic matter	−26.94	685±21	0±30	0–10
PLD-7925	59–60	Organic matter	−26.57	3222±29	2537±36	2480–2650
PLD-7495	69–70	Organic matter	−27.73	3630±27	2945±34	2970–3220
PLD-7926	79–80	Organic matter	−26.72	4034±30	3349±37	3470–3690
PLD-7927	89–90	Organic matter	−25.40	4575±31	3890±37	4230–4430
PLD-7496	101–102	Organic matter	−28.38	5304±27	4619±34	5290–5470

[a] Laboratory code of of Paleo Labo Co., Ltd., Japan.

[b] The reservoir correction factor is 685±21 yr, ^{14}C age of the uppermost 1 cm of the core sediments.